

Degeneration and Regeneration of Corneal Nerves in Response to HSV-1 Infection

Ana J. Chucair-Elliott,¹ Min Zheng,¹ and Daniel J. J. Carr^{1,2}

¹Department of Ophthalmology, University of Oklahoma Health Sciences Center, Oklahoma City, Oklahoma, United States

²Department of Microbiology and Immunology, University of Oklahoma Health Sciences Center, Oklahoma City, Oklahoma, United States

Correspondence: Ana J. Chucair-Elliott, Department of Ophthalmology, University of Oklahoma Health Sciences Center, 608 Stanton L. Young Boulevard, Oklahoma City, OK 73104, USA; ana-chucair@ouhsc.edu.

Submitted: September 2, 2014

Accepted: December 20, 2014

Citation: Chucair-Elliott AJ, Zheng M, Carr DJJ. Degeneration and regeneration of corneal nerves in response to HSV-1 infection. *Invest Ophthalmol Vis Sci.* 2015;56:1097-1107. DOI:10.1167/iovs.14-15596

PURPOSE. Herpes simplex virus type 1 (HSV-1) infection is one cause of neurotrophic keratitis, characterized by decreases in corneal sensation, blink reflex, and tear secretion as consequence of damage to the sensory fibers innervating the cornea. Our aim was to characterize changes in the corneal nerve network and its function in response to HSV-1 infection.

METHODS. C57BL/6J mice were infected with HSV-1 or left uninfected. Corneas were harvested at predetermined times post infection (pi) and assessed for β III tubulin, substance P, calcitonin gene-related peptide, and neurofilament H staining by immunohistochemistry (IHC). Corneal sensitivity was evaluated using a Cochet-Bonnet esthesiometer. Expression of genes associated with nerve repair was determined in corneas by real time RT-PCR, Western blotting, and IHC. Semaphorin 7A (SEMA 7A) neutralizing antibody or isotype control was subconjunctivally administered to infected mice.

RESULTS. The area of cornea occupied by β III tubulin immunoreactivity and sensitivity significantly decreased by day 8 pi. Modified reinnervation was observed by day 30 pi without recovery of corneal sensation. Sensory fibers were lost by day 8 pi and were still absent or abnormal at day 30 pi. Expression of SEMA 7A increased at day 8 pi, localizing to corneal epithelial cells. Neutralization of SEMA 7A resulted in defective reinnervation and lower corneal sensitivity.

CONCLUSIONS. Corneal sensory nerves were lost, consistent with loss of corneal sensation at day 8 pi. At day 30 pi, the cornea reinnervated but without recovering the normal arrangement of its fibers or function. SEMA 7A expression was increased at day 8pi, likely as part of a nerve regeneration mechanism.

Keywords: corneal nerves, HSV-1, neurotrophic keratitis, reinnervation, semaphorin 7A

The cornea is the most densely innervated tissue of the body. Its fibers, mostly sensory in origin and derived from the ophthalmic branch of the trigeminal nerve, enter peripherally parallel to the corneal surface. These nerves lose their perineuria and myelin sheaths close to the limbus and continue to advance toward the center of the tissue as they subdivide into smaller and more superficial branches. Eventually, a sub-basal nerve plexus is formed with nerve endings that penetrate the corneal epithelium.¹⁻³ Corneal fibers form the afferent arm of reflexes for blinking and tearing by sensing thermal, mechanical, and chemical stimuli that cause the release of crucial soluble factors for maintenance of wound healing and homeostasis of the ocular surface.^{1,4,5} Because the integrity of the cornea relies on a competent nerve supply, the structural patterns of its nerves, including density, number, degree of branching, and tortuosity, have clinical relevance.^{4,6} Dysfunction of corneal innervation is a feature frequently associated with noninfectious and infectious inflammatory corneal diseases leading to a degenerative condition known as neurotrophic keratitis (NTK). Noninfectious causes of NTK include trigeminal nerve damage associated with orbital or head injury, head trauma, aneurysms, or intracranial neurologic disease.^{7,8} In addition, dry eye symptoms related to NTK have been

described in laser vision correction with laser in situ keratomileusis (LASIK),⁹ longstanding use of contact lenses,¹⁰ and diabetes mellitus.^{11,12} Herpetic viral infections of the ocular surface such as herpes simplex virus type 1 (HSV-1), the leading cause of infectious corneal blindness in the industrialized world,^{13,14} are thought to be a major cause of the development of NTK.^{7,15,16} HSV-1 enters into a host cell through a multistep process as a result of fusion between the viral envelope and target plasma membrane through the interactions of the HSV-1-encoded glycoproteins gB, gD, gH, and gL, with their cognate receptors.¹⁷ Shortly after replicating at the initial site of infection, the virus uses retrograde axonal transport to gain access to the sensory neurons in the trigeminal ganglia, where it establishes latent infection.¹⁸ Upon reactivation, newly created particles of virus travel down sensory trigeminal nerve fibers to epithelial surfaces where they replicate locally. Chronic episodes of viral reactivation followed by corneal infection can lead to herpes stromal keratitis (HSK), characterized by tissue damage, opacity elicited by episodic immune responses,¹⁹⁻²¹ and vascularization of the normally avascular cornea.²²⁻²⁴ HSK is associated with development of NTK, playing a role in the diagnosis and prognosis of all types of herpetic keratitis. The loss of corneal sensation in HSK patients,

often assessed by loss of a corneal blink reflex, is strongly correlated with profound loss of the sub-basal nerve plexus.²⁵

The causes and consequences of corneal damage, as well as corneal nerve regeneration processes upon HSV-1 infection have been poorly explored and fit within the National Eye Institute's scope of interest, as highlighted by the Cornea Disease Panel, in its August 2012 Vision Research: Needs, Gaps, and Opportunities compendium (<https://www.nei.nih.gov/sites/default/files/nei-pdfs/VisionResearch2012.pdf>). Therefore, in the present study, we aimed to characterize changes in corneal innervation during acute and latent HSV-1 infection as well as mechanisms of nerve regeneration upon infection. Previous reports have indicated the regenerative response following nerve injury includes the expression of neurotrophins, regeneration-associated genes (RAGS) and gene products such as growth-associated protein-43 (GAP43)^{26,27} and nerve guidance molecules from the semaphorin (SEMA) family, such as SEMA 3A²⁸ and SEMA 7A.²⁹ Particular attention was focused on SEMA 7A, the only glycosylphosphatidylinositol-linked semaphorin that promotes axonal outgrowth and regeneration and recruits inflammatory cells^{29,30} by integrin-mediated signaling.^{30,31}

We found that in response to HSV-1 infection, sensory nerves and corneal sensitivity were lost within 8 days post infection (pi), followed by aberrant nerve regeneration without functional recovery, as observed at 30 days pi, a time point consistent with latent infection. HSV-1 induced up-regulation of the expression of SEMA 7A in corneal epithelial cells, consistent with nerve fiber loss. Furthermore, neutralization of SEMA 7A resulted in hyperinnervation at the center of the cornea with impaired corneal sensation. We interpret these results to suggest SEMA 7A is part of the nerve damage-regeneration mechanism following HSV-1 infection.

METHODS

Animals

All animal procedures were approved by the University of Oklahoma Health Sciences Center and Dean McGee Eye Institute Institutional Animal and Care and Use Committee and were performed in adherence to the Association for Research in Vision and Ophthalmology Statement for the Use of Animals in Ophthalmic and Vision research. C57BL/6 mice were obtained from Jackson Laboratory (Bar Harbor, ME, USA). Mice were 6 to 8 weeks old at the time experiments were performed.

Virus and In Vivo Infection

HSV-1 strain McKrae was propagated on HSV-1-susceptible green monkey kidney (Vero) cells and maintained at a stock concentration of 10⁸ plaque-forming units (PFU)/mL. Anesthetized mice were infected by scarification of the corneal surface, followed by application of 3.0 μ L of PBS containing virus (10⁵ PFU/eye) as previously described.³² Controls were created by scarifying corneas and/or leaving them uninfected (UI).

Viral Plaque Assay

At indicated time points, corneas were homogenized, clarified by centrifugation (10,000g for 1.5 minutes), and then serially diluted and poured onto a confluent lawn of Vero cells in RPMI 1640 medium (Invitrogen, Life Sciences, Grand Island, NY, USA) containing 10% fetal bovine serum (FBS) and antibiotic/antimycotic reagents (Invitrogen). Plaques were visualized and enumerated with the aid of an inverted microscope (Invertoskop; Zeiss, Thornwood, NY, USA) 24 hours later and

quantified as mean log PFU per cornea as previously described.³³

Corneal Sensitivity

As previously published,³⁴ a Cochet-Bonnet esthesiometer (catalog no. 8630-1490-29; Luneau SAS, France) was used to test for corneal sensitivity. Briefly, at different times pi, nonanesthetized mice were held by the scruff of the neck and presented with a monofilament at lengths ranging from 6.0 to 0.5 cm in 0.5-cm fractions to elicit a blink response. At each length, the monofilament touched the cornea four times, making perpendicular contact with the surface before considering a response negative (no blink response). The lack of blink reflex at a monofilament length of 0.5 cm was recorded as 0. All measurements were performed by the same examiner.

Neutralization of SEMA 7A

At 7 days pi, deeply anesthetized mice received subconjunctival injections of 5 μ g of anti-SEMA 7A antibody or isotype-labeled control antibody (rat IgG_{2B}) to both eyes (10 μ L; catalog nos. MAB2068 and MAB0061, respectively; R&D Systems, Minneapolis, MN, USA), using a 31-gauge syringe under a dissecting scope. Injections were repeated every 3 days, and mice were kept in the vivarium until cornea tissue was collected at 24 days pi.

Immunohistochemistry and Imaging

For immunohistochemistry (IHC), at indicated times pi, mice were anesthetized and transcardially perfused with PBS. Eyes were removed and an incision was made posterior to the limbus in order to dissect the corneas including a margin of sclera. Corneas were fixed with 4% paraformaldehyde for 30 minutes, followed by a permeation step consisting of three washes with 1% Triton X-100 (Triton)/PBS for 15 minutes. Samples were then blocked overnight with 10% normal donkey serum (NDS) in 0.1% Triton/PBS, followed by overnight incubation with primary antibodies. Following overnight incubation, the samples were washed 3 \times with 0.1% Triton/PBS for 30 minutes, incubated with fluorescent-labeled secondary antibody for 1 hour (1:150 dilution), stained with nuclear dye (4',6-diamidino-2-phenylindole [DAPI]) and washed 3 \times with 0.1% Triton/PBS for 30 minutes. Incisions were made in each cornea in order to obtain a flower-shaped whole mount (four quadrants) prior to mounting in 50% glycerol for imaging. Following fixation, some corneas were cryoprotected by overnight incubation with 30% sucrose and then frozen in optimal cutting temperature medium (catalog no. 4583; Tissue-Tek, Torrance, CA, USA). Corneal cryostat sections (14 μ m) were rinsed with 1% Triton/PBS, blocked with 10% NDS/PBS, and immunostained. The primary antibodies used were anti- β III tubulin (catalog no. 18207; 1:1000 dilution; Abcam, Cambridge, MA, USA), anti-neurofilament heavy chain (NFH; catalog no. PA3-16753; 1:500 dilution; Thermo Scientific, Pittsburgh, PA, USA), anti-substance P (SP; catalog no. 556312; 1:200 dilution; BD Pharmingen, San Diego, CA, USA), anti-calcitonin gene-related protein (CGRP; catalog no. 1720-9007; 1:200 dilution; AbD Serotec, Raleigh, NC, USA), anti-CD45 (catalog no. 550539; 1:200 dilution; BD Pharmingen), and anti-CD31 (catalog no. MAB1398Z; 1:100 dilution; Millipore, Billerica, MA, USA). All fluorescently labeled secondary antibodies were purchased from Jackson Laboratories (Jackson ImmunoResearch, West Grove, PA, USA). Imaging was performed using an MVX10 imaging system for whole-cornea flat-mounts (cellSens Dimension 1.8.1; Olympus, Center Valley, PA, USA) and a FluoView confocal laser scanning

microscope for cornea quadrant captures (FV500; version 5.0; Olympus). Microscope and software settings were identical for all samples within experiments. To quantify changes in corneal innervation, MetaMorph version 7.7.0.0 offline software (Molecular Devices, LLC, Sunnyvale, CA, USA) was used to calculate the percentage of threshold area positive for β III tubulin staining on acquired confocal images, defined as the percentage of β III tubulin⁺ pixels divided by the total number of pixels per field of view. For each cornea, a representative image from each quadrant was used for analysis (four images per sample where the visual field included the peripheral limbus toward the center of the cornea proper). The summary was used to generate the percentage of threshold area positive for β III tubulin staining per sample. At least 4 replicates from 3 independent experiments were used per time point. In experiments comparing the changes in corneal innervation in the center of the tissue, a single representative image of the central cornea per sample was captured in at least 6 corneas per group from 2 independent experiments. For a three-dimensional view of the corneal innervation, representative images captured as above were processed using Fluoview viewer (FV 10-ASW 4.0 v; Olympus).

Real Time RT-PCR

At different times pi, total RNA from two corneas was extracted with TRIzol reagent (catalog no. 15596018; Ambion, Life Sciences, Grand Island, NY, USA) and converted to cDNA (iScript reverse transcription supermix; Bio-Rad Laboratories, Hercules, CA, USA) as previously described.²² Transcript levels of GAP43, SEMA 3A, SEMA 7A, and eukaryotic translation elongation factor 1 epsilon-1 (Eef1e1, a housekeeping gene) were measured using iQSYBR Green PCR Supermix and a CFX96 real-time PCR detection system (Bio-Rad Laboratories). Primer sequences for GAP43, SEMA 3A, SEMA 7A, and Eef1e1 (IDT Integrated DNA Technologies, Coralville, IA, USA) were as follows: GAP43 forward (5'-TGGTGTCAAGCCGGAAGATAA-3') and GAP43 reverse (5'-GCTGGTGCATCACCTTCT-3'); SEMA 3A forward (5'-GAAGAGCCCTTATGATCCCAAAC-3') and SEMA 3A reverse primer (5'-AGATAGCGAAGTCCCGTCCC-3'); SEMA 7A forward (5'-ACACACCGTGCTTTCCATGA-3') and SEMA 7A reverse (5'-CCTTTGTGGAGCCGATGTTTC-3'); and Eef1e1 forward (5'-GCAGAAGAAAAGGCAATGGT-3') and Eef1e1 reverse (5'-AGGCCGTAGTACAGCAGGAT-3'). Relative quantities of gene expression were calculated by the comparative C_T value method,³⁵ and the results were expressed as fold change of expression for each transcript.

Western Blotting

At indicated time points following infection, corneas were harvested, pooled (2 to 3 corneas/sample), and lysed with radioimmunoprecipitation assay lysis buffer (catalog no. sc-24948; Santa Cruz Biotechnology, Inc., Dallas, TX, USA). Protein content was measured using a BCA protein assay (catalog no. 23225; Thermo Scientific). Equal amounts of protein were resolved on SDS-4% to 20% gradient polyacrylamide gels (catalog no. EC60285; Invitrogen) and transferred onto nitrocellulose membranes. Proteins were detected using the primary antibodies anti- β III tubulin (catalog no. ab18207; 1:2000 dilution; Abcam), anti-SEMA 7a (catalog no. ab23578; 1:200; Abcam), and anti- β actin (catalog no. ab6276; 1:10,000; Abcam). For secondary chemiluminescent detection, blots were incubated with corresponding horseradish-peroxidase-conjugated secondary antibodies (GE Healthcare Bio-Sciences, Pittsburgh, PA, USA). Imaging of blots and analysis of bands intensities were performed by conventional image analysis using in vivo imaging system F Pro (Kodak, Rochester, NY,

USA) and MI SE 4.4 SE version software (Carestream Health, Inc., Rochester, NY, USA).

Statistical Analysis

Statistical analysis was performed by using Prism version 5.0 software (GraphPad software, San Diego, CA, USA). Data are means \pm SEM for each group. The unpaired *t*-test was performed to assess significant differences ($P < 0.05$) among groups. For multiple comparisons, one-way analysis of variance was performed followed by the Newman-Keuls post hoc test.

RESULTS

HSV-1 Infection Results in Deinnervation and Subsequent Reinnervation of the Cornea

The normal cornea is the most densely innervated tissue in the human body¹ yet is devoid of blood or lymphatic vessels. Angiogenesis of blood and lymphatic vessels^{22,23} along with nerve damage and loss of corneal sensation^{36,37} represent important pathogenic mechanisms of HSK, likely due to HSV-1 neurotropism and the elicited immune response. To study the effect of HSV-1 infection on the structure and function of corneal nerves and its temporal relationship with HSV-1-induced angiogenesis, C57BL6 mice eyes were infected with 10⁵ PFU HSV-1 or were left UI as controls, as previously described.³² In this model, acute infection within the cornea was resolved by approximately 10 days pi,^{20,38-40} followed by a latent phase of infection within the sensory neurons in the trigeminal ganglia.^{20,22} In order to study innervation during acute and latent infection, at different time points, including 2, 4, 6, and 8 days pi (acute), as well as 14 and 30 days pi (latent), mice were euthanized and their corneas harvested and processed for IHC staining with an antibody against the pan-neuronal marker β III tubulin and an antibody against CD31, an endothelial cell marker. As previously described for normal corneas,^{1,3,36} UI corneas displayed intact innervation consisting of a stromal network formed by thick nerve trunks that ramified into smaller and more superficial branches as they progressed from the periphery toward the center of the cornea (Fig. 1; Supplementary Fig. S1). A sub-basal network composed of thinner hairpin-like nerves that projected centripetally and presented a roughly parallel orientation from one another, terminating in free nerve endings, was observed (Fig. 1A, G-G"; Fig. 2, C2). As seen in representative corneal whole-mount images (Figs. 1A-C) in comparison to the UI condition, HSV-1 infection resulted in the loss of corneal nerves that was more pronounced in the center at 8 days pi (Fig. 1B). A reinnervation process was evident at 30 days pi (Fig. 1C). A unique feature often observed in corneas at 30 days pi was abnormal and disorganized hyperinnervation in the center of the tissue (Fig. 1C). For greater structural detail and quantitative assessment of the effect of HSV-1 on the extent of the nerve network, confocal images were taken from cornea quadrants (Figs. 1G-M"). Compared to UI corneas and corneas at 2 days pi displaying intact stromal and sub-basal innervation (Fig. 1D, yellow arrows: thick stromal nerves and white arrows: thin sub-basal nerve bundles; Figs. 1, G-G", H-H"), HSV-1 infection caused progressive loss of nerves starting at 4 days pi, with near complete loss of the sub-basal plexus by day 8 pi (Figs. 1K-K"). Although reinnervation was evident by 30 days pi (Figs. 1, L-L", M-M"), areas with no sub-basal hairpin-like nerves were observed. Corneal innervation quantified as the percentage of threshold area positive for β III tubulin signal in representative confocal images showed statistically significant decreases in the area of tissue innervation at days 6, 8, and 14

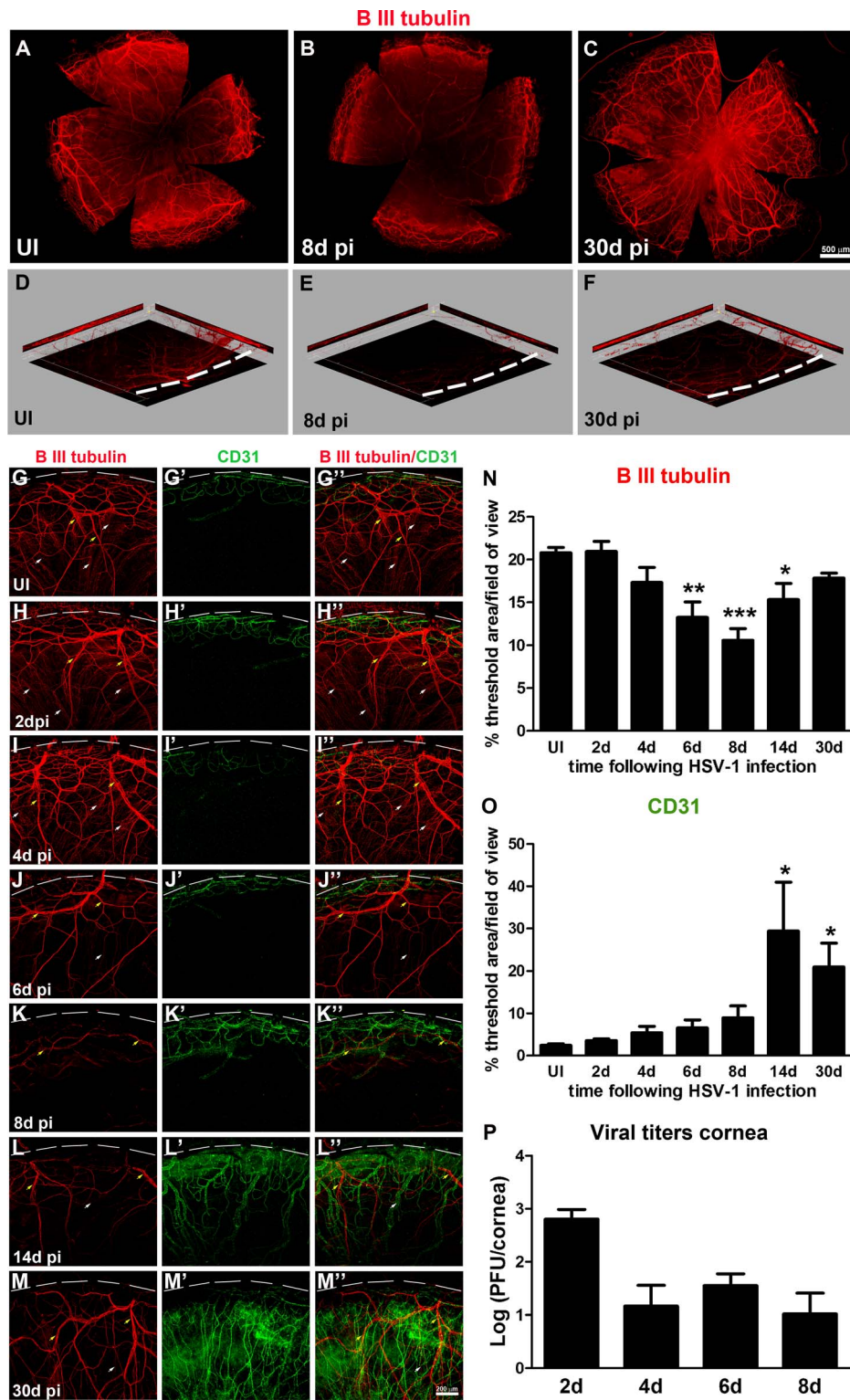


FIGURE 1. HSV-1 infection results in deinnervation and subsequent reinnervation, consistent with progressive neovascularization of the cornea. Mouse eyes were infected with 10^3 PFU of HSV-1 or left UI as controls. At 2, 4, 6, 8, 14, and 30 days pi, corneas were processed for IHC staining with β III tubulin (red) and CD31 (green) antibodies. (A–C) Representative corneal whole-mount images. In comparison to UI (A), displaying intact corneal innervation, HSV-1 infection resulted in loss of corneal nerves more pronounced in the center of a 6- and 8-day pi (B) and in the reinnervation process evident at 30 days pi (C). A unique feature observed in some corneas at 30 days pi was abnormal and disorganized hyperinnervation in the center of the tissue. (D–F) Three-dimensional view of representative images showing loss of overall innervation at day 8 pi (E) and regaining innervation at day 30 pi (F). Notice the red signal from β III tubulin-stained nerves, absent throughout the thickness of the optical section (E), and nerve recovery (F). (G–M'') Representative confocal images of UI and infected cornea quadrants oriented with the limbal margins at the top (white dashed lines). Compared to UI (G–G'') displaying intact innervation with thick stromal nerves (yellow arrows) and fine sub-basal nerve bundles (white arrows), HSV-1 infection caused progressive loss of nerves and complete loss of sub-basal nerves at day 8 pi, consistent with the onset of neovascularization of the cornea (K–K''). This event was followed by reinnervation that coexisted with persistent neovascularization

(L-L', M-M'). Corneal innervation and neovascularization were quantified as percentage of threshold area positive for β III tubulin signal (N) and for CD31 signal (O) in representative confocal images (G-M'). Bars represent the percentage of threshold area/field of view \pm SEM ($n =$ at least 4 total replicates from 3 independent experiments for each group in (N); and $n =$ at least 3 replicates from 2 independent experiments for each group in (O)). * $P < 0.01$; ** $P < 0.001$; *** $P < 0.0001$, compared to UI group as determined by ANOVA followed by Newman-Keuls multiple comparison test. (P) Viral content in corneas at 2, 4, 6, and 8 days pi as assessed by viral plaque assay and expressed as log (PFU/cornea) \pm SEM ($n = 6$ total replicates from 2 independent experiments per time point).

pi (Fig. 1N). A three-dimensional view of representative images showed intact fine bundles of nerves positive for β III tubulin in the UI condition, which were completely lost by day 8 pi and partially recovered at 30 days pi (Figs. 1D-F).

Recently published work suggests the loss of nerves in the cornea resulted in the disruption of the corneal vascular privilege.⁴¹ Of interest, at 8 days pi, when the maximum loss of nerves occurred, HSV-1-induced neovessels started to invade the cornea proper (Figs. 1K'-K''), consistent with a mutual inhibition effect between nerves and vessels. However, at 14 days pi, when the reinnervation of the cornea appeared to be triggered, the area of the neovascularized cornea was increased and remained significantly elevated at 30 days pi (Figs. 1, L'-L'', M'-M'', O). Corneal nerve retraction was observed when infectious virus could be isolated from cornea tissue (Fig. 1P). However, at time points consistent with viral resolution, the cornea recovered innervating fibers that coexisted with pathological vascularization.

HSV-1 Infection Results in Loss of Corneal Sensory Fibers and a Deficient or Abnormal Reinnervation Process

The normal cornea contains extensive and complex peptidergic innervation composed of nociceptive CGRP- and SP-positive fibers⁴² with some myelinated, non-nociceptive peripheral nerves¹ that stain positive for NFH.⁴³ To evaluate the qualitative changes in corneal nerves upon HSV-1 infection, mouse eyes were infected or left UI as controls. Corneas were then processed for IHC and stained with antibodies against β III tubulin with either SP, CGRP, or NFH at times pi (Fig. 2). As observed in sagittal frozen sections of corneas costained with β III tubulin and SP, both periphery (Figs. 2A1, A3, A5) and center (Figs. 2A2, A4, A6) corneal tissue showed β III tubulin⁺ nerves in the stroma and rich sub-basal innervation penetrating the layers of epithelial cells that colocalized with expression of SP. Loss of sub-basal innervation was observed at 8 days pi (Figs. 2A7-12) with remaining peripheral nerves that did not colocalize with SP (Figs. 2A7, A9, A11). Reinnervation of the cornea at 30 days pi (Figs. 2A13-18) involved poor sub-basal reinnervation and hyperinnervation of the central stroma without recovery of SP expression. Cornea sections costained with β III tubulin and CGRP (Figs. 2B1-18) showed constitutive CGRP expression mostly within the epithelial cells (Figs. 2B1-6) and was occasionally associated with nerves at the sub-basal and stromal locations. At 8 days pi, CGRP expression remained in the epithelium but was not associated with remaining nerves at the peripheral cornea (Figs. 2B7-12). In fact, there was an up-regulation of expression in the central cornea compared to UI and 30-day-pi corneas. At day 30 pi, CGRP expression was found in some of the nerves that reinnervated the stroma (Figs. 2B13-18). Analysis of NFH immunostaining in cornea whole mounts revealed hyperinnervation at the center of the tissue at 30 days pi that included the abnormal presence of NFH⁺ nerves (3 of 12 corneas). In summary, HSV-1 infection induced a dramatic regression of sensory fibers by day 8 pi. This process was followed by aberrant nerve regeneration with an absence of fibers at the sub-basal and epithelial locations. The pathological response also

included abnormal reinnervation of the central stroma characterized by loss of expression of SP and occasionally NFH⁺ myelinated nerves.

Nerve Regression Following HSV-1 Infection Results in Loss of Corneal Sensitivity Without Recovery Upon Corneal Reinnervation

Anatomical nerve regeneration is not, in all cases, associated with functional recovery. To determine whether the loss of innervation induced by HSV-1 infection correlated with loss of nerve function, mice infected with 10^3 PFU HSV-1 were monitored for corneal sensitivity at 5, 8, 21, and 30 days pi. Because successful HSV-1 infection in the cornea requires gently scratching the epithelial surface to generate a lesion for virus penetrance at this challenge dose, parallel sham controls were performed in which mice were scarified but were UI. In addition, a control group was not subjected to the scarification procedure and were left UI (naive). Corneas from all control mice (UI and naive) exhibited maximum corneal sensitivity, with Cochet-Bonnet scale values close to 6 cm (100% sensitivity) (Fig. 3). In contrast, at 5 days pi, a subtle reduction of function was recorded that became statistically significant at 8 days pi, consistent with maximum structural nerve loss (Fig. 3). Despite the reinnervation process, by day 30 pi, corneal sensation did not recover.

SEMA 7A Expression in the Cornea Is Elevated Upon HSV-1 Infection and Plays a Role in the Reinnervation Process

To study the mechanism behind the deinnervation-reinnervation processes in the cornea following HSV-1 infection, the expression levels of some regeneration-associated genes and guidance molecule candidates previously found to be significantly expressed in models of corneal nerve transection^{29,43} and transplantation²⁸ were measured. Mice were ocularly infected with 10^3 PFU HSV-1 or left UI as controls or were not subjected to the scarification procedure (naive). At different time points (2, 6, and 8 days pi), corneas were harvested and processed for RNA isolation and cDNA synthesis to specifically focus on the expressions of GAP43, SEMA 3A, and SEMA 7A. Real time PCR analysis did not show statistically significant levels of expression among the three candidate genes between groups at any time point studied (Figs. 4A-C). However, because a strong trend toward elevation of SEMA 7A transcript was observed at 8 days pi, we pursued SEMA 7A expression at the protein level and its localization in the cornea. Densitometric analysis of immunoblots showed SEMA 7A protein expression was significantly elevated in infected corneas compared to that in the UI condition at day 8 pi, detected mostly as a glycosylated form of SEMA 7A (~100 kDa), as previously observed⁴⁴ (Figs. 4D, 4E). This observation correlated with a significant decrease in β III tubulin protein levels at 8 days pi due to nerve loss (Figs. 4D, 4F).

SEMA 7A is expressed by several pre- and postnatal neuronal populations,^{30,45} as well as by a broad variety of lymphoid and myeloid cells.⁴⁶⁻⁴⁸ In the naive cornea, SEMA 7A expression was recently localized to epithelial and stromal

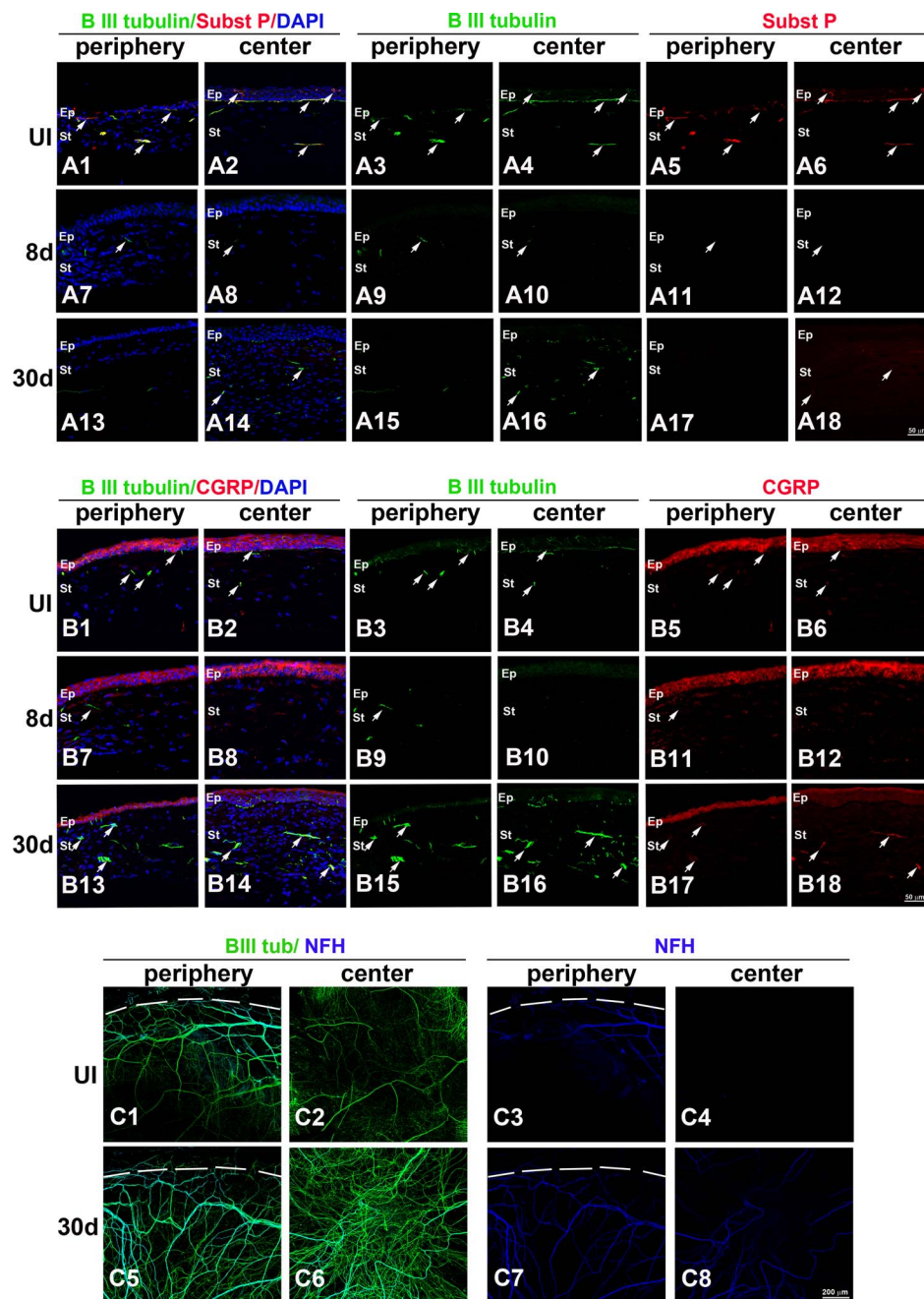


FIGURE 2. HSV-1 infection results in loss of corneal sensory fibers and a deficient or abnormal reinnervation process. Mouse eyes were infected with 10^3 PFU HSV-1 or left UI as controls. At 8 and 30 days pi, corneas were processed for IHC costaining with β III tubulin (green) with SP (red), CGRP (red), or NFH (blue) antibodies. (A1–A18) Sagittal frozen sections of corneas costained with β III tubulin and SP. In the UI cornea, both periphery (A1, A3, A5) and center (A2, A4, A6) showed β III tubulin⁺ nerves in the stroma and rich subbasal innervation penetrating the layers of epithelial cells that colocalized with expression of SP (white arrows). Loss of sub-basal innervation was observed at 8 days pi (A7–A12) with remaining peripheral nerves that did not colocalize with SP (A7, A9, A11). The reinnervation of the cornea at 30 days pi (A13–A18) involved poor sub-basal reinnervation and hyperinnervation of the central stroma without recovery of SP⁺ signal (white arrows). (B1–B18) Sagittal frozen sections of corneas costained with β III tubulin and CGRP. In the UI cornea, CGRP expression was found mostly within the epithelial cells (B1–B6) and was occasionally associated with nerves at the sub-basal and stromal locations. At 8 days pi, CGRP continued to be expressed in the epithelium and was not associated with remaining nerves at the peripheral cornea (B7–B12). At day 30 pi, CGRP reactivity at the central epithelium region was largely lost, whereas some of the nerves that reinnervated the stroma colocalized with CGRP expression (B13–B18). (C1–C8) Corneal whole mounts show hyper-reinnervation at the center of the cornea at 30 days pi that included the abnormal presence of NFH⁺ nerves. DAPI, nuclei counterstain in blue; Ep, epithelium; St, stroma. Figure represents $n = 3$ mice/time point or UI controls from two independent experiments.

cells.²⁹ To determine whether the source of SEMA 7A increase in the infected corneas was resident cells or infiltrating immune cells or both, costaining of corneal cross sections was performed using antibodies against SEMA 7A and CD45 (Figs. 4G–J). IHC analysis revealed constitutive expression of

SEMA 7A by corneal epithelial cells, detected in a weak, punctate pattern. Following 8 days pi, SEMA 7A staining was more robust and was evident on the cell membrane of corneal epithelial cells and extremely faint or absent in CD45⁺ inflammatory cells or keratocytes. Protein analysis of SEMA

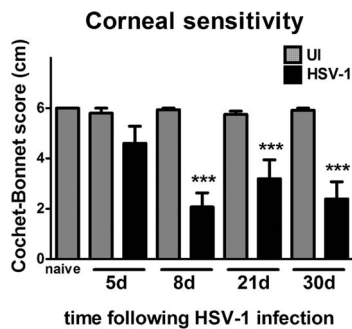


FIGURE 3. Corneal reinnervation following HSV-1 infection does not correlate with recovery of corneal sensitivity. Mouse eyes were infected with 10^5 PFU HSV-1, were left UI as controls, or were not subjected to the scarification procedure (naive). At 5, 8, 21, and 30 days pi, corneal sensitivity levels were measured by Cochet-Bonnet esthesiometer and compared among groups. At day 8 pi, there was a significant loss of corneal sensitivity recorded in corneas of infected mice that did not recover by day 30 pi. Bars represent average Cochet-Bonnet score \pm SEM (n = at least 10 for the HSV-1 groups and n = at least 6 for the UI groups from 2 independent experiments). *** P < 0.0001 compared to UI group at each time point as determined by ANOVA followed by Newman-Keuls multiple comparison test.

7A in parallel to that of β III tubulin was also conducted at 5 days and 30 days pi with no significant differences between infected and uninfected groups at both time points (data not shown). We interpret the results to suggest the increase of SEMA 7A was time-dependent and required nerve loss as a stimuli.

In order to address whether the up-regulation of SEMA 7A following HSV-1 infection played a role in reinnervation of the cornea, the effect of local neutralization of SEMA 7A in the cornea on the regeneration of the corneal nerve network and its function upon infection was studied. Taking into account the fact that the significant increase of corneal SEMA 7A protein was observed at 8 days pi, subconjunctival delivery of anti-SEMA 7A or matching isotype control (IgG_{2B}) antibody was initiated at 7 days pi and continued until 24 days pi. At that time point, mice were subjected to cornea sensitivity measurements, and their corneas were harvested and processed for IHC analysis of nerves (Fig. 5). As revealed by β III tubulin immunostaining of corneal whole mounts, infected corneas treated with anti-SEMA 7A antibody (HSV-1⁺ α SEMA 7A) exhibited central areas with disorganized hyperinnervation that lacked fine sub-basal nerve bundles in comparison to their isotype controls in which the regenerating nerves adopted a centripetal orientation (HSV-1⁺ isotype; compare Figs. 5B-F with Figs. 5A-D). In both treatments, the innervation was similar at the peripheral locations (compare Figs. 5B-E with Figs. 5A-C). Corneal innervation measured as the percentage of threshold area positive for β III tubulin signal showed no changes at the peripheral cornea, but there was a significant increase in the positive area occupied by nerves in the center of anti-SEMA 7A antibody-treated corneas. Measurement of corneal sensitivity showed significant impairment in anti-SEMA 7A antibody-treated corneas compared to isotype-treated controls. The loss of corneal sensation was likely a consequence of the loss of intraepithelial free nerve endings in the central cornea along with stromal hyperinnervation.

DISCUSSION

Our study provides a longitudinal characterization of the changes in corneal innervation network following HSV-1 infection and explores a mechanism for corneal nerve

regeneration with potential clinical relevance in the treatment of neuropathy of the ocular surface. First, we found HSV-1 infection caused a dramatic regression of sensory afferents innervating the cornea, mostly SP⁺ and CGRP⁺ nociceptive fibers during acute infection accompanied by the loss of corneal sensitivity. At later time points, once the viral infection of the tissue was cleared, the cornea reinnervated but often without readopting the normal arrangement of its fibers, peptidergic content, or function. Our results suggest the up-regulation of SEMA 7A is induced by nerve loss and plays a role in the reinnervation process following HSV-1 infection.

Corneal sensory nerves release a variety of biologically active neurochemicals on which the healthy state of the cornea depends. Large numbers of these fibers contain SP and/or CGRP, two neuropeptides with described roles in epithelial renewal and wound repair.^{1,49} Physiologically relevant concentrations of SP are found in the normal cornea and tears, which have been reported to decrease following surgical deinnervation and neonatal capsaicin treatment,^{50,51} as well as in patients with herpetic keratitis.⁵¹ A reduction in SP content in HSK corneas is not surprising considering the profound loss of the sub-basal nerve plexus loss associated with a reduction in corneal sensation found in patients following HSV infection.^{25,52} Such findings in human patients are in agreement with the results in our model. We found uninfected mouse corneas exhibit rich sub-basal innervation, with nerve endings penetrating the epithelium that stain positive for SP. HSV-1 infection caused massive nerve regression with almost complete loss of the sub-basal nerve plexus and SP reactivity. Of interest, despite the reinnervation observed at 30 days pi with a prominent presence of fibers in the middle and posterior stroma at the center of the cornea, neither the fine nerve bundles at the subepithelial location nor SP reactivity were recovered. In uninfected and infected corneas, CGRP reactivity was strong in epithelial cells, which might be explained as released neuropeptide bound to CGRP receptors, abundantly expressed on corneal and limbal epithelial cells.^{53,54} In our hands, the detection of CGRP in nerves was scarce, limited to occasional subepithelial and stromal fine fibers that were absent at 8 days pi. At 30 days pi, CGRP reactivity was increased within stromal nerves normally not observed in uninfected corneas. In addition to the described changes in peptidergic fibers, areas of central stromal hyperinnervation contained NFH⁺ fibers, corresponding to myelinated afferents. The presence of myelinated fibers in the central corneal stroma is abnormal and has also been reported in the context of corneal nerve regeneration following surgical nerve transection.⁴³ The functional significance of such fibers during reinnervation is not known.

In addition to its effect on nerves, HSV-1 infection causes the pathological growth of blood and lymphatic vessels into the normally avascular cornea.²²⁻²⁴ The maximum nerve loss observed in our model coincided with the onset of neovascularization in response to HSV-1 infection, which fits the paradigm that vessels and nerves maintain “cross-talk” to inhibit each other in the cornea.⁴¹ However, this was not the case by 30 days pi or even 3 to 4 months pi (preliminary data not shown), as regenerated nerves were present, coexisting with highly vascularized tissue. It is tempting to speculate that following infection, the infiltration of inflammatory cells and their products, induced by angiogenesis as well as factors released through the “leaky” neovessel walls, could influence the regeneration of damaged/regressed nerves leading to the abnormal structural features and loss of sensitivity of the corneal nerve network described above.

Our data suggest that up-regulation of SEMA 7A, a nerve guidance factor that stimulates axonal growth and proper axon track formation during development,^{30,44,45} is a likely compo-

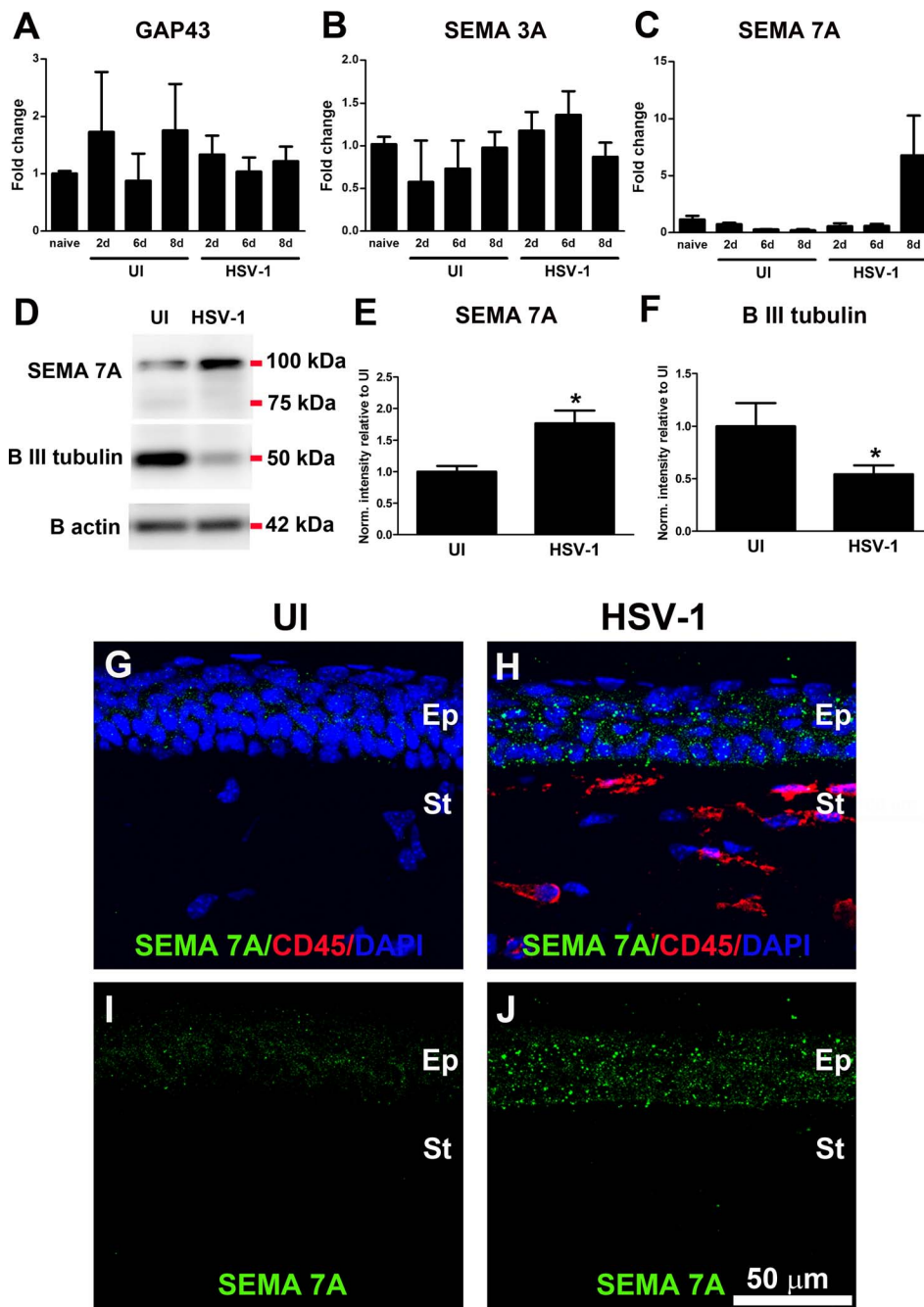


FIGURE 4. HSV-1 infection of the cornea induces up-regulation of SEMA 7A. Mouse eyes were infected with 10^3 PFU HSV-1, left UI as controls, or were not subjected to the scarification procedure (naive). (A–C) At 2, 6, and 8 days pi, corneas were harvested and processed for RNA isolation, followed by cDNA synthesis and real time RT-PCR analysis of genes associated with nerve damage or regeneration. (A) GAP43, (B) SEMA 3A, and (C) SEMA 7A. Although no significant changes were observed in the expression of GAP43 and SEMA3A transcripts, a strong trend toward increase in SEMA 7A was observed at day 8 pi ($n =$ at least 3 replicates for each group from 2 independent experiments for GAP43 and SEMA 3A and from 1 experiment for SEMA 7A analyzed by ANOVA). (D) Representative blots from protein extracts in which infected corneas showed significant increase in SEMA 7A content, consistent with decreased content of β III tubulin at 8 days pi. (E, F) Densitometric analysis of SEMA 7A and β III tubulin proteins. Internal normalizations were done for β actin (loading control), and results are normalized intensity values relative to mean UI \pm SEM ($n = 4$ for UI and $n = 7$ for HSV-1 groups from 2 independent experiments; $*P < 0.05$ as determined by unpaired t -test). (G–J) Representative confocal images of frozen cross-sections of corneas immunostained with SEMA 7A (green) and CD45 (red) antibodies. At day 8 pi, the constitutive expression of SEMA 7A was increased mostly in epithelial cells. Faint or absent staining was found within stromal and/or inflammatory cells. DAPI, nuclei counterstain in blue; Ep, epithelium; St, stroma. Images are representative for two corneas/mice per group.

ment of the nerve regeneration response in the cornea upon HSV-1 infection. Localization of SEMA 7A expression in the cornea and its role in nerve regeneration and inflammation have been explored in the context of lamellar corneal surgery.²⁹ Specifically, constitutive expression of SEMA 7A in

the corneal epithelial cells and to a lesser extent in stromal keratocytes was up-regulated within stromal cells near the regenerating nerve fronds following surgery.²⁹ In a similar manner, we found SEMA 7A expression concentrated in the corneal epithelium in the uninfected corneas. However,

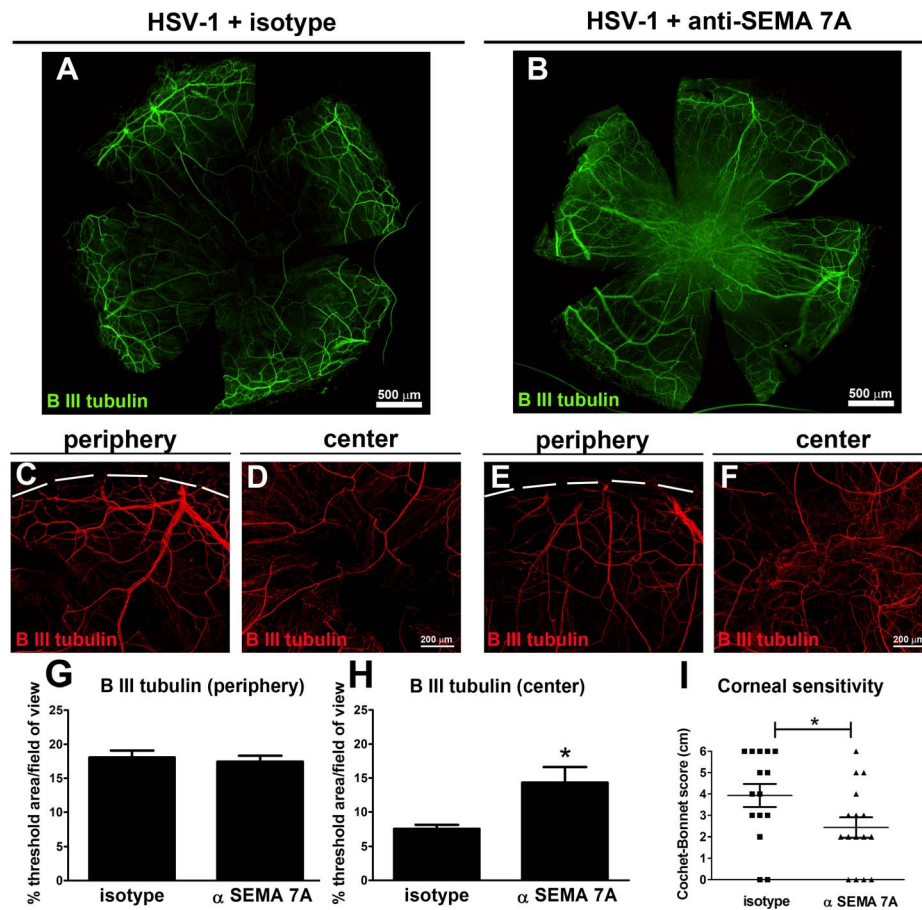


FIGURE 5. Neutralization of SEMA 7A affects reinnervation of the central cornea and decreases corneal sensitivity. Mice were infected with 10^3 PFU of HSV-1 in their corneas and at day 7 pi were given subconjunctival doses of 5 μ g of anti-SEMA 7A or isotype control (IgG_{2B}) antibody at repeated doses every 3 days. At 24 days pi, mice were subjected to cornea sensitivity measurements, and their corneas were harvested and processed for IHC analysis. (A, B) Representative β III tubulin staining of cornea whole mount from infected mouse treated with isotype (HSV-1+ isotype) (A) or with anti-SEMA 7A (B) antibody shows aberrant innervation at the *center* of the anti-SEMA 7A-treated corneas. In the *peripheral area*, confocal images show nerves (red) recovered to a similar extent in isotype- (C) and anti-SEMA 7A antibody-treated (E) corneas. At the *center*, the anti-SEMA 7A antibody-treated corneas show aberrant hyperinnervation (F) compared to isotype-treated corneas (D). (G, H) Corneal innervation was quantified as percentage of threshold area positive for β III tubulin signal in representative confocal images (C–F). Bars represent the percentage of threshold area/field of view \pm SEM ($^*P < 0.05$; $n = 11$ for (G) and $n = 12$ total replicates per group for (H) from two independent experiments). (I) At 24 days pi, corneal sensitivity levels were measured by a Cochet-Bonnet esthesiometer and compared among groups. Corneal sensitivity was significantly impaired in anti-SEMA 7A antibody-treated corneas compared to that in isotype-treated mice by an unpaired *t*-test ($^*P < 0.05$). Individual scores recorded for each individual cornea with their respective average \pm SEM per experimental group are indicated in the graph ($n = 11$ for HSV-1+ isotype; and $n = 12$ for HSV-1+ anti-SEMA 7A from two independent experiments).

increased expression localized to the epithelium was evident 8 days pi with weak or absent expression in keratocytes or CD45⁺ cells. Because earlier or later time points (5 and 30 days pi) did not show significant changes in the expression of SEMA 7A relative to their uninfected counterparts, we interpret the time of maximum nerve regression was key to orchestrate the SEMA 7A response by epithelial cells to guide or stimulate the outgrowth of nerve terminals as a mechanism of nerve regeneration. We report that most of the infected corneas that received subconjunctival delivery of anti-SEMA 7A antibody exhibited aberrant innervation at 24 days pi (14 of 16 total corneas) involving areas with misguided arrangement of stromal hyperinnervation and scarce or absent sub-basal nerves (11 of 16 total corneas). Such aberrant features were observed in only 2 of 15 total isotype control antibody-treated corneas. Consistent with the more abnormal nature of nerve regeneration upon anti-SEMA 7A antibody administration, the corneal sensation was significantly decreased in mice under this treatment compared to the isotype control-treated mice. Moreover, the innervation pattern of infected corneas treated

with the isotype IgG_{2B} did not match the one observed in infection-only corneas. Generally, isotype control antibody-treated corneas displayed a “healthier” pattern of reinnervation, with more frequent areas of short fine nerve bundles and less frequent central hyperinnervation than the infection-only cornea group (13.3% vs. 25%). However, both groups of mice had average corneal sensitivity values similar to each other and significantly lower than uninfected corneas (comparison shown in Supplementary Fig. S3). In the nervous and immune systems, SEMA 7A is thought to bind to plexin C1 and β 1 integrin receptors.^{30,31} However, in various tissues, including the cornea, the significance of these interactions is poorly understood. In addition to roles in modulating the nervous and immune systems, SEMA 7A has also been linked to vascular growth in corneal neovascularization.⁵⁵ In their work, Ghanem et al.⁵⁵ showed mouse corneas injected with naked SEMA 7A cDNA developed neovascularization in comparison to vector-treated controls. In contrast, we showed a strong trend toward elevation of neovascularization in corneas treated with anti-SEMA 7A in comparison to isotype-treated corneas following

HSV-1 infection (Supplementary Fig. S2). It is hard to extrapolate our findings to those of Ghanem et al.⁵⁵ as different model systems were used. Nevertheless, both studies convey the capacity of SEMA 7A to regulate the vascular system in the cornea.

Mechanistic evidence behind the nerve regression following HSV-1 infection of the cornea is lacking. Recent work has proposed the loss of corneal sensitivity and blink reflex due to HSV-1-induced nerve damage led to desiccation of the ocular surface and exacerbation of inflammation.³⁷ The recovery of the structure and function of corneal nerves was found to be negatively impacted by CD4⁺ T cells,³⁷ which suggests that the persistent and selective presence of an inflammatory phenotype in the cornea following HSV-1 infection can account for long-term nerve damage, including a loss of corneal sensation. The cause of corneal nerve degeneration following HSV-1 infection remains unclear but likely involves the immune system³⁷ and events that transpire within the sensory ganglion.

Acknowledgments

The authors thank Blake Hopiavuori, Xiaowu Gu, and Alex Cohen for technical assistance, and Michael Elliott for critical comments during the preparation of the manuscript.

Supported by National Institutes of Health Grant R01 EY021238, an Oklahoma Center for Adult Stem Cell Research (OCASCR) grant through the Oklahoma Tobacco Settlement Endowment Trust, and an unrestricted grant from Research to Prevent Blindness.

Disclosure: **A.J. Chucair-Elliott**, None; **M. Zheng**, None; **D.J.J. Carr**, None

References

- Muller LJ, Marfurt CF, Kruse F, Tervo TM. Corneal nerves: structure, contents and function. *Exp Eye Res.* 2003;76:521-542.
- Radner W, Mallinger R. Interlacing of collagen lamellae in the midstroma of the human cornea. *Cornea.* 2002;21:598-601.
- Shaheen BS, Bakir M, Jain S. Corneal nerves in health and disease. *Surv Ophthalmol.* 2014;59:263-285.
- Beurman RW, Schimmelpennig B. Sensory denervation of the rabbit cornea affects epithelial properties. *Exp Neurol.* 1980;69:196-201.
- Marfurt CF, Cox J, Deek S, Dvorscak L. Anatomy of the human corneal innervation. *Exp Eye Res.* 2010;90:478-492.
- Seyed-Razavi Y, Chinnery HR, McMenamin PG. A novel association between resident tissue macrophages and nerves in the peripheral stroma of the murine cornea. *Invest Ophthalmol Vis Sci.* 2014;55:1313-1320.
- Davis EA, Dohlman CH. Neurotrophic keratitis. *Int Ophthalmol Clin.* 2001;41:1-11.
- Paton L. The trigeminal and its ocular lesions. *Br J Ophthalmol.* 1926;10:305-342.
- Linna TU, Vesaluoma MH, Perez-Santonja JJ, Petroll WM, Alio JL, Tervo TM. Effect of myopic LASIK on corneal sensitivity and morphology of subbasal nerves. *Invest Ophthalmol Vis Sci.* 2000;41:393-397.
- Patel SV, McLaren JW, Hodge DO, Bourne WM. Confocal microscopy in vivo in corneas of long-term contact lens wearers. *Invest Ophthalmol Vis Sci.* 2002;43:995-1003.
- Lockwood A, Hope-Ross M, Chell P. Neurotrophic keratopathy and diabetes mellitus. *Eye (Lond).* 2006;20:837-839.
- Rosenberg ME, Tervo TM, Immonen IJ, Muller LJ, Gronhagen-Riska C, Vesaluoma MH. Corneal structure and sensitivity in type 1 diabetes mellitus. *Invest Ophthalmol Vis Sci.* 2000;41:2915-2921.
- Howard M, Sellors JW, Jang D, et al. Regional distribution of antibodies to herpes simplex virus type 1 (HSV-1) and HSV-2 in men and women in Ontario, Canada. *J Clin Microbiol.* 2003;41:84-89.
- Looker KJ, Garnett GP. A systematic review of the epidemiology and interaction of herpes simplex virus types 1 and 2. *Sex Transm Infect.* 2005;81:103-107.
- Cavanagh HD, Pihlaja D, Thoft RA, Dohlman CH. The pathogenesis and treatment of persistent epithelial defects. *Trans Sect Ophthalmol Am Acad Ophthalmol Otolaryngol.* 1976;81:754-769.
- Liesegang TJ. Corneal complications from herpes zoster ophthalmicus. *Ophthalmology.* 1985;92:316-324.
- Karasneh GA, Shukla D. Herpes simplex virus infects most cell types in vitro: clues to its success. *Virology.* 2011;8:481.
- Miller CS, Danaher RJ, Jacob RJ. Molecular aspects of herpes simplex virus I latency, reactivation, and recurrence. *Crit Rev Oral Biol Med.* 1998;9:541-562.
- Biswas PS, Banerjee K, Kinchington PR, Rouse BT. Involvement of IL-6 in the paracrine production of VEGF in ocular HSV-1 infection. *Exp Eye Res.* 2006;82:46-54.
- Carr DJ, Harle P, Gebhardt BM. The immune response to ocular herpes simplex virus type 1 infection. *Exp Biol Med (Maywood).* 2001;226:353-366.
- Wickham S, Carr DJ. Molecular mimicry versus bystander activation: herpetic stromal keratitis. *Autoimmunity.* 2004;37:393-397.
- Wuest TR, Carr DJ. VEGF-A expression by HSV-1-infected cells drives corneal lymphangiogenesis. *J Exp Med.* 2010;207:101-115.
- Zheng M, Schwarz MA, Lee S, Kumaraguru U, Rouse BT. Control of stromal keratitis by inhibition of neovascularization. *Am J Pathol.* 2001;159:1021-1029.
- Zheng M, Deshpande S, Lee S, Ferrara N, Rouse BT. Contribution of vascular endothelial growth factor in the neovascularization process during the pathogenesis of herpetic stromal keratitis. *J Virol.* 2001;75:9828-9835.
- Hamrah P, Cruzat A, Dastjerdi MH, et al. Corneal sensation and subbasal nerve alterations in patients with herpes simplex keratitis: an in vivo confocal microscopy study. *Ophthalmology.* 2010;117:1930-1936.
- Chaudhary S, Namavari A, Yco L, et al. Neurotrophins and nerve regeneration-associated genes are expressed in the cornea after lamellar flap surgery. *Cornea.* 2012;31:1460-1467.
- Huebner EA, Strittmatter SM. Axon regeneration in the peripheral and central nervous systems. *Results Probl Cell Differ.* 2009;48:339-351.
- Omoto M, Yoshida S, Miyashita H, et al. The semaphorin 3A inhibitor SM-345431 accelerates peripheral nerve regeneration and sensitivity in a murine corneal transplantation model. *PLoS One.* 2012;7:e47716.
- Namavari A, Chaudhary S, Ozturk O, et al. Semaphorin 7a links nerve regeneration and inflammation in the cornea. *Invest Ophthalmol Vis Sci.* 2012;53:4575-4585.
- Pasterkamp RJ, Peschon JJ, Spriggs MK, Kolodkin AL. Semaphorin 7A promotes axon outgrowth through integrins and MAPKs. *Nature.* 2003;424:398-405.
- Suzuki K, Okuno T, Yamamoto M, et al. Semaphorin 7A initiates T-cell-mediated inflammatory responses through alpha1beta1 integrin. *Nature.* 2007;446:680-684.
- Conrady CD, Zheng M, Fitzgerald KA, Liu C, Carr DJ. Resistance to HSV-1 infection in the epithelium resides with the novel innate sensor, IFI-16. *Mucosal Immunol.* 2012;5:173-183.

33. Austin BA, Halford WP, Williams BR, Carr DJ. Oligoadenylate synthetase/protein kinase R pathways and alphabeta TCR+ T cells are required for adenovirus vector: IFN-gamma inhibition of herpes simplex virus-1 in cornea. *J Immunol.* 2007;178:5166-5172.
34. Cortina MS, He J, Russ T, Bazan NG, Bazan HE. Neuroprotectin D1 restores corneal nerve integrity and function after damage from experimental surgery. *Invest Ophthalmol Vis Sci.* 2013;54:4109-4116.
35. Chucair-Elliott AJ, Elliott MH, Wang J, et al. Leukemia inhibitory factor coordinates the down-regulation of the visual cycle in the retina and retinal-pigmented epithelium. *J Biol Chem.* 2012;287:24092-24102.
36. Gallar J, Tervo TM, Neira W, et al. Selective changes in human corneal sensation associated with herpes simplex virus keratitis. *Invest Ophthalmol Vis Sci.* 2010;51:4516-4522.
37. Yun H, Rowe AM, Lathrop KL, Harvey SA, Hendricks RL. Reversible nerve damage and corneal pathology in murine herpes simplex stromal keratitis. *J Virol.* 2014;88:7870-7880.
38. He J, Ichimura H, Iida T, et al. Kinetics of cytokine production in the cornea and trigeminal ganglion of C57BL/6 mice after corneal HSV-1 infection. *J Interferon Cytokine Res.* 1999;19:609-615.
39. Jung HW, Jung CR, Choi BK, et al. Herpesvirus infection of ICAM-1-deficient mice. *Curr Eye Res.* 2004;29:201-208.
40. Pasiacka TJ, Cilloniz C, Lu B, et al. Host responses to wild-type and attenuated herpes simplex virus infection in the absence of Stat1. *J Virol.* 2009;83:2075-2087.
41. Ferrari G, Hajrasouliha AR, Sadrai Z, Ueno H, Chauhan SK, Dana R. Nerves and neovessels inhibit each other in the cornea. *Invest Ophthalmol Vis Sci.* 2013;54:813-820.
42. Jones MA, Marfurt CF. Peptidergic innervation of the rat cornea. *Exp Eye Res.* 1998;66:421-435.
43. Namavari A, Chaudhary S, Sarkar J, et al. In vivo serial imaging of regenerating corneal nerves after surgical transection in transgenic thy1-YFP mice. *Invest Ophthalmol Vis Sci.* 2011;52:8025-8032.
44. Sultana H, Neelakanta G, Foellmer HG, et al. Semaphorin 7A contributes to West Nile virus pathogenesis through TGF-beta1/Smad6 signaling. *J Immunol.* 2012;189:3150-3158.
45. Xu X, Ng S, Wu ZL, et al. Human semaphorin K1 is glycosylphosphatidylinositol-linked and defines a new subfamily of viral-related semaphorins. *J Biol Chem.* 1998;273:22428-22434.
46. Holmes S, Downs AM, Fosberry A, et al. Sema7A is a potent monocyte stimulator. *Scand J Immunol.* 2002;56:270-275.
47. Mine T, Harada K, Matsumoto T, et al. CDw108 expression during T-cell development. *Tissue Antigens.* 2000;55:429-436.
48. Sato Y, Takahashi H. Molecular cloning and expression of murine homologue of semaphorin K1 gene. *Biochim Biophys Acta.* 1998;1443:419-422.
49. Garcia-Hirschfeld J, Lopez-Briones LG, Belmonte C. Neurotrophic influences on corneal epithelial cells. *Exp Eye Res.* 1994;59:597-605.
50. Keen P, Tullo AB, Blyth WA, Hill TJ. Substance P in the mouse cornea: effects of chemical and surgical denervation. *Neurosci Lett.* 1982;29:231-235.
51. Yamada M, Ogata M, Kawai M, Mashima Y. Decreased substance P concentrations in tears from patients with corneal hypesthesia. *Am J Ophthalmol.* 2000;129:671-672.
52. Cruzat A, Witkin D, Baniyadi N, et al. Inflammation and the nervous system: the connection in the cornea in patients with infectious keratitis. *Invest Ophthalmol Vis Sci.* 2011;52:5136-5143.
53. Heino P, Oksala O, Luhtala J, Uusitalo H. Localization of calcitonin gene-related peptide binding sites in the eye of different species. *Curr Eye Res.* 1995;14:783-790.
54. Tran MT, Ritchie MH, Lausch RN, Oakes JE. Calcitonin gene-related peptide induces IL-8 synthesis in human corneal epithelial cells. *J Immunol.* 2000;164:4307-4312.
55. Ghanem RC, Han KY, Rojas J, et al. Semaphorin 7A promotes angiogenesis in an experimental corneal neovascularization model. *Curr Eye Res.* 2011;36:989-996.